



Original article

Effect simultaneous delivery with P-glycoprotein inhibitor and nanoparticle administration of doxorubicin on cellular uptake and in vitro anticancer activity



Ozgur Esim^a, Meral Sarper^b, Cansel K. Ozkan^a, Sema Oren^b, Baris Baykal^c, Ayhan Savaser^{a,*}, Yalcin Ozkan^a

^a University of Health Sciences, Gulhane Faculty of Pharmacy, Department of Pharmaceutical Technology, Ankara, Turkey

^b University of Health Sciences, Gulhane Institute of Health Sciences, Ankara, Turkey

^c University of Health Sciences, Gulhane Faculty of Medicine, Department of Histology and Embryology, Ankara, Turkey

ARTICLE INFO

Article history:

Received 1 November 2019

Accepted 12 February 2020

Available online 17 February 2020

Keywords:

Doxorubicin

Verapamil

P-glycoprotein

Nanoparticle

ABSTRACT

Multidrug resistance (MDR) is the most common problem of inadequate therapeutic response in tumor cells. Many trials has been developed to overcome drug efflux by P-glycoprotein (P-gp). For instance, co-administration of a number of drugs called chemosensitizers or MDR modulators with a chemotherapeutic agent to inhibit drug efflux. But for optimal synergy, the drug and inhibitor combination may need to be temporally colocalized in the tumor cells. In this study, we encapsulated the Ver and Dox in PLGA nanoparticles to inhibit the P-gp drug efflux in breast cancer. Moreover, the effect of either Dox solution (Dox_S), Dox nanoparticles (Dox_{NP}), Dox_S + Ver_S, Dox_{NP} + Ver_S, Dox_{NP} + Ver_{NP} or Dox-Ver_{NP} was evaluated. It was found that co administration of Dox_{NP} with Ver_{NP} (70.76%) showed similar cellular uptake of Dox to Dox/Ver combination solution (70.62%). However it is observed that Dox_{NP} + Ver_{NP} has the highest apoptotic activity (early apoptotic 13.52 ± 0.06%, late apoptotic 53.94 ± 0.15%) on human breast adenocarcinoma (MCF 7) cells. Hence, it is suggested that Dox_{NP} + Ver_{NP} is a promising administration for tumor therapy.

© 2020 Published by Elsevier B.V. on behalf of King Saud University. This is an open access article under the CC BY-NC-ND license (<http://creativecommons.org/licenses/by-nc-nd/4.0/>).

1. Introduction

Chemotherapy has been the first choice in the treatment of many cancer types (e.g., breast cancers) for many years, still, inadequate therapeutic responses can occur. The most common problem for this inadequate therapeutic response is multidrug resistance (MDR) which is generally related with upregulation of an ATP-dependent efflux pump permeability-glycoprotein (P-gp) (Wu et al., 2007). P-gp is a membrane-related glycoprotein that can efflux numerous substrates, with a diversity of chemotherapeutic agents to outside of plasma membrane, which decreases intracellular drug quantity. Since chemotherapeutic agents have many dose-limiting side effects, it is usually unfeasible to over-

come P-gp drug efflux simply by using the chemotherapeutic agents at higher concentration. Therefore it is essential to use alternative methods to enhance the treatment rate of chemotherapy (Wong et al., 2006). Paragraph: use this for the first paragraph in a section, or to continue after an extract.

Until now, diversity of trials has been developed to overcome drug efflux by P-gp. For instance, co-administration of a number of drugs called chemosensitizers or MDR modulators with a chemotherapeutic agent to inhibit drug efflux (Alkhaith and Al-Saedi, 2017; Dönmez et al., 2011; Qin et al., 2014; Shafiei-Irannejad et al., 2018; Song et al., 2009; Wang et al., 2005; Wu et al., 2007). These drugs do not show any cytotoxic effect alone but they can upregulate the chemotherapeutic agents by reversing the P-gp-related MDR (Dönmez et al., 2011). Verapamil (Ver) is one of the most popular drugs with a P-gp inhibitory activity. However the dose required for Pgp blockade (2–6 μM) of Ver is higher than its clinical dose (0.4–1.2 mM) and at higher doses Ver may induce cardiotoxicity. Moreover, P-gp expression is also observed in healthy tissue cells (J. Wang et al., 2005). Thus, an additional approach must be used to inhibit the P-gp drug efflux without unwanted side effects (Wu et al., 2007).

* Corresponding author.

E-mail address: ayhan.savaser@sbu.edu.tr (A. Savaser).

Peer review under responsibility of King Saud University.



Nanoparticles are gaining great attention with their small sizes, enhanced circulation times and sustained drug release in physiological conditions. Also chemotherapeutic agent loaded nanoparticles can improve the anticancer efficacy while reducing the unwanted side effects (Luo et al., 2010). Nevertheless, the sustained release of nanoparticles are commonly very slow and cannot be precisely controlled thus therapeutic concentrations may not be maintained in treatment of diseases (Wu et al., 2007). Moreover, although it is shown that nanoparticles overcome the drug efflux, at higher resistance levels such as in tumors, particulate drug delivery systems may not circumvent P-gp significantly by themselves (J. Wang et al., 2005). Hence, the co-encapsulation of a chemotherapeutic agent and a chemosensitizer has been widely investigated and polymeric nanoparticles (Alkhaitb and Al-Saedi, 2017), liposomes (Wang et al., 2005), and solid lipid nanoparticles (SLNs) (Baek and Cho, 2015) offer great potential to succeed the aforementioned aim (Wong et al., 2006).

Doxorubicin (Dox) has been used for the treatment of many cancer types including breast cancer for many years (Kauffman et al., 2016). However, the clinical application of doxorubicin is limited by its MDR and unwanted side effects. So, several studies have focused on different approaches to deliver Dox to the tumor side efficiently (Luo et al., 2010) such as the co-delivery of Dox and Ver using various particulate drug delivery systems, including liposomes (Wang et al., 2005), solid lipid nanoparticles (Wong et al., 2004), hydrogel (Qin et al., 2014) and polymeric nanoparticles (Khdair et al., 2009) on different cancer types. Results showed that co-delivery of a chemotherapeutic agent and a chemosensitizer in nanoparticles offer a great potential for overcoming tumor MDR (Qin et al., 2014; Wu et al., 2007).

In this study, we encapsulated the Ver and Dox in PLGA nanoparticles to inhibit the P-gp drug efflux in breast cancer. Moreover, the effect of either Dox solution (Dox_S), Dox nanoparticles (Dox_{NP}), Dox_S + Ver_S, Dox_{NP} + Ver_S, Dox_{NP} + Ver_{NP} or Dox-Ver_{NP} was evaluated. The characterization and anticancer effects of the prepared nanoparticles were evaluated using MCF 7 cell line. To compare the controlled and immediate release of both cytotoxic agent (Dox) and P-gp inhibitor (Ver) on cytotoxicity profile, we used real time cytotoxicity measurement system. Compared to other cytotoxicity measurement methods, real time cell monitoring systems offer time dependent profile of cytotoxicity which is an important parameter especially for controlled release products. We also demonstrated the enhanced anticancer effects of Ver and Dox loaded nanoparticles on MCF 7 cell lines.

2. Materials and methods

2.1. Materials

Verapamil hydrochloride, PLGA (Resomer RG 504 H) and Polyvinyl alcohol (Mowiol 4-88) were procured from Sigma Aldrich (USA). Doxorubicin Hydrochloride was a gift from Deva, Turkey. Annexin V-FITC and propidium iodide were obtained from Serva, Germany. All other reagents and chemicals used were of analytical grade.

2.2. Methods

2.2.1. Preparation of PLGA nanoparticles

DOX_{NP}, Ver_{NP} and Dox-Ver_{NP} were prepared by previously reported emulsification solvent evaporation method with minor modifications (Mobarak et al., 2014). In brief, 3 mg of Dox and/or Ver was dissolved in 1 mL 1% PVA solution (pH 7.0) and sonicated with dichloromethane containing PLGA (90 mg/3 mL) using a probe sonicator at 30 W for 60 s (Sonopuls, Bandelin, Germany).

Resulting emulsion was further mixed with 10 mL 1% PVA solution under sonication at 50 W for 60 s followed by solvent evaporation using rotary evaporator (Buchi R 215, Germany). Obtained nanodispersion was purified using centrifuge at 10,000 rpm for 15 min. Pellet was washed and redispersed in water and centrifuged three times. Obtained suspension was lyophilized at -80 °C for 72 h (Christ, Gamma 2-20, USA)

2.2.2. Physical characterization

The particle size and polydispersity index (PDI) of prepared nanoparticles was determined by PCS (Nicomp Nano Z3000, PSS, USA). The size measurements were done at triplicate and results were expressed as z-average size ± S.D. Morphological analysis of prepared nanoparticles was done using scanning electron microscopy (SEM) (Zeiss Evo 40, Germany). The photographs were taken at 100,000× magnification and 10 kV voltage. The zeta (ζ) potential was measured by Laser Doppler Velocimetry (PSS Nicomp Nano Z3000 particle size analyzer (PSS, USA)) at 25°C. Values are presented as mean ± S.D. from three replicates. The encapsulation efficiency (EE%) of Dox_{NP}, Ver_{NP} and Dox-Ver_{NP} were determined after complete dissolution in dichloromethane. The solutions were passed through a membrane filter (pore size 0.22 μm, Millipore, Darmstadt, Germany) and determined by HPLC (Agilent 1100, CA, USA).

2.2.3. HPLC analysis

Quantitative estimation of Dox and Ver were done by an in house developed HPLC method. The system equipped with DAD and FLD detector (Agilent 1100, CA, USA) was used for the analysis of samples. Separation was achieved with mobile phase consisting of 0.05 M potassium dihydrogen phosphate buffer and acetonitrile (80:20 v/v) using C8 analytical column (4.6 × 150 mm, 5 μm, Agilent, USA) at the flow rate of 1 mL/min and column temperature 25 °C. Analysis was carried out at 210 nm for Ver and 480 nm excitation and 550 nm emission for Dox.

2.2.4. In vitro drug release study

The release pattern of Dox and Ver from nanoparticles were calculated using dialysis method (cut-off 12–14 kDa, Spectrum Labs, USA) in PBS pH 7.4 as a medium in a constant temperature shaker (Nuve, Ankara, Turkey) at 70 rpm. 1 mL each of nanoparticle dispersion was placed in dialysis bags and both ends of the bags were sealed. The bags were placed into 20 mL 20 mL receptor medium (PBS pH 7.4). At predetermined time intervals samples were withdrawn and replenishment of receptor compartment with same volume of fresh dialyzing medium was done. Analysis was done in triplicate. Results were calculated as cumulative drug release % versus time.

2.2.5. Cell culture study

RPMI 1640 with 1% penicillin G streptomycin and 10% fetal bovine serum (Gibco BRL, Grand Island, NY) were used to grow MCF 7 cells which were provided from American Type Culture Collection (ATCC, Manassas, VA). Cells were grown at 37 °C in a humidified, 5% CO₂ atmosphere.

2.2.5.1. Electrical impedance based real-time cytotoxicity assay. xCELLigence (ACEA Biosciences, Inc., San Diego, CA) cell monitoring system was used to determine the changes in the cell viability. 16 well plate with an array of gold electrodes were used for monitoring the real time cell behavior by calculating the changes in the electric impedance (Martinez-Serra et al., 2014; Ozdemir and Ark, 2013). 50 μl DMEM were poured into each well and background signals were measured. After background measurement MCF 7 cells were seeded into each well in 100 μl cell suspension at a density of 15 × 10⁻³ per well. The plates were stored for

20 min for homogenous sedimentation of cells and wells were mounted on monitoring unit and placed in CO₂ incubator and cells was monitored at 37 °C overnight. After observing the plateau on cell monitoring system, wells were removed and 50 µl of aliquot was replaced with same volume of DMEM containing drug nanoparticles and/or drug solutions. Cell index (CI) which expresses the electrical impedance signal was automatically recorded in every 15 min for next 72 h to obtain the cell viability. Experiment was done in triplicate (Muckova et al., 2019).

2.2.5.2. Cell uptake study. Dox uptake by MCF 7 cells treated Dox_S, Dox_{NP}, Dox_S + Ver_S, Dox_{NP} + Ver_S, Dox_{NP} + Ver_{NP} or Dox-Ver_{NP} was determined qualitatively and quantitatively by fluorescence microscopy and FACS. For determination of doxorubicin uptake by cells quantitatively, cells were incubated with the 10 µM Dox and or 9.5 µM Ver/well for different time intervals (1, 2, 4 h). After incubation, cells were washed three times with ice cold PBS 7.4, trypsinized and centrifuged for 3 min at 3000 rpm. Obtained cell suspension was analyzed by fluorescence activated cell sorter (FACS) (Beckman Coulter, Moflo Astrios, USA). Totally 10,000 cells per sample were analyzed and each experiment was done in triplicate.

Moreover, the uptake of Dox by MCF 7 cells were visualized by fluorescent microscopy. 1×10^5 cell were seeded in each well of 24-well plate and cells were allowed to attach for 24 h. After 24 h the medium was replaced with Dox_S, Dox_{NP}, Dox_S + Ver_S, Dox_{NP} + Ver_S, Dox_{NP} + Ver_{NP} or Dox-Ver_{NP} (10 µM Dox and or 9.5 µM Ver/well) solution or suspensions and wells were incubated for 1 h. In given time point, the medium was removed and cells were washed with ice cold PBS 7.4 thrice and fixed. The nuclei of the cells were stained with Hoechst 33258 nuclear stain diluted (1/1000) in PBS. Cells were visualized using a fluorescence microscope (DMI6000, Leica, Germany) equipped with Sytox Blue HC-Filterset (Leica, Germany) for Hoechst 33258 and HQ-Filterset for Alexa 546 for Dox.

2.2.5.3. Cell death analysis. The MCF 7 cells at a density of 1×10^5 cells per well were incubated overnight, treated with treatment with Dox_S, Dox_{NP}, Dox_S + Ver_S, Dox_{NP} + Ver_S, Dox_{NP} + Ver_{NP} or Dox-Ver_{NP} (Untreated cells were used as controls) at the end of incubation and incubated again for 24 h. After 24 h, the cells were washed, trypsinized and suspended in fresh medium. The suspension was centrifuged at 2500 rpm for 6 min. Obtained cell pellets were resuspended in Annexin V binding buffer and centrifuged in same conditions. Cell pellets (1×10^5 /mL) were stained with AnnexinV-FITC and PI and analyzed by flow cytometer (Moflo Astrios, Beckman Coulter, USA). The results were expressed as four different cell populations as viable (AnnexinV-FITC (-), PI (-)), early apoptotic (AnnexinV-FITC (+), PI (-)), late apoptotic (AnnexinV-FITC (+), PI (+)) and necrotic (AnnexinV-FITC (-), PI (+)). The calculated results were given as bar chart indicating the respective percentages of each group and the cell percentages were determined by software.

2.3. Statistical analysis

All experiments were done in triplicate and results were expressed as the mean ± standard deviation. Student's *t*-test and ANOVA was used to determine differences between results. Results with *P*-values <0.05 were considered statistically significant ($\alpha = 0.05$).

3. Results and discussion

In this study, we compared the effect of single or co-delivery of Dox and Ver as nanoparticle and/or drug solution. In accordance with this aim, our primary approach was to prepare Dox_{NP}, Ver_{NP} and Dox-Ver_{NP} efficiently. Nanoparticles were prepared by a W/O/W double emulsification solvent evaporation method which is used commonly for entrapment of water soluble drugs (Alkhaib and Al-Saedi, 2017; Song et al., 2009). Dox and Ver encapsulation efficiencies were found 43.1 ± 1.37 and $45.6 \pm 2.44\%$, respectively after single entrapment of drugs. PLGA forms a negatively charged nanoparticles thus allows the incorporation of cationic drugs (Qin et al., 2014; Song et al., 2010). Due to Dox and Ver are cationic weakly basic drugs, it is possible to load both drugs into anionic PLGA nanoparticles. Previously, preparation of different nanosized systems co-loaded with Dox and Ver were described (Qin et al., 2014; Wang et al., 2005; Wu et al., 2007). Also it has recently been shown that PLGA nanoparticles can be used for the co-loading of drugs (Song et al., 2010). In this study, we showed that Dox and Ver co-loaded PLGA nanoparticles can be prepared effectively. The encapsulation efficiency of prepared Dox-Ver_{NP} was found $40.2 \pm 1.37\%$ for Dox and $38.1 \pm 1.96\%$ for Ver which is close to encapsulation efficiency of single drug loaded nanoparticles (Table 1) ($p > 0.05$). The different encapsulation efficiencies of drugs are due to their different solubility properties of Dox and Ver (H. Wang et al., 2011).

Dynamic Light Scattering (DLS) analysis results showed that the mean diameter of nanoparticles were 198.3 ± 3.5 nm for Dox_{NP}, 228.1 ± 17.1 nm for Ver_{NP} and 289.5 ± 25.71 nm for Dox-Ver_{NP}. (Table 1). The particle size of Dox-Ver_{NP} was bigger than that of Dox_{NP} and Ver_{NP} ($p < 0.05$), probably resulting from the higher total drug content. The phenomenon that increase in total loaded drug content could improve the particle size and polydispersity index has been also reported in the previous articles (Soni et al., 2015). The polydispersity index (PDI), identified by the percentages of the coefficient of variation (CV%), was around the 0.1 for the Ver_{NP} and Dox_{NP} indicating a great normal size distribution of the nanoparticles, whereas the PDI of the Dox-Ver_{NP} was moderate around 0.225 (Alkhaib and Al-Saedi, 2017). As displayed in Fig. 1, all of the Dox_{NP} (Fig. 1a), Ver_{NP} (Fig. 1b) and Dox-Ver_{NP} (Fig. 1c) were spherical. However, the particle sizes varied by the change in the composition of formulations as demonstrated in Table 1.

3.1. In vitro drug release study

Drug release from PLGA nanoparticles were calculated due to the drug release profiles of drugs are correlated with their therapeutic efficacy. In drug release profiles, an initial burst release was observed for 2 h which can be attributed to the release of drug that attached on the surface of nanoparticles (Mulik et al., 2010). After 6 h, the release profile was found steadier indicating the sustained drug release from nanoparticles. The cumulative Dox release percentage after 24 h was $83 \pm 1.46\%$ for Dox_{NP} and $75 \pm 2.33\%$ for Dox-Ver_{NP} and Ver release after 24 h was $88 \pm 2.14\%$ for Ver_{NP} and $81 \pm 2.02\%$ for Dox-Ver_{NP}.

The most interesting finding in this study was that cumulative drug release from co-loaded nanoparticles was lower than the single drug loaded nanoparticles. This phenomenon was also confirmed by other studies. When the drugs were co-encapsulated in the nanoparticle formulations, the release of both drugs were slower than their single drug loaded nanoparticles. Interestingly, the Dox had a similar release for Dox_{NP} and Dox-Ver_{NP} in first 8 h but slower than the rest. Based on the shape of the curve, it is found that both drugs have a slower release in Dox-Ver_{NP}. More-

Table 1
Physical characteristics of nanoparticles.

	Particle size (nm)	PDI	Zeta potential (mV)	Encapsulation efficiency (%)
DOX _{NP}	198.3 ± 3.5*	0.125 ± 0.08	-13.6 ± 0.26	43.1 ± 1.37
Ver _{NP}	228.1 ± 17.1*	0.068 ± 0.06	-17.5 ± 0.58	45.6 ± 2.44
Dox-Ver _{NP}	289.5 ± 25.7	0.225 ± 0.11	-20.5 ± 1.53	40.2 ± 1.37–38.1 ± 1.96

* Significantly different from Dox-Ver_{NP} (p < 0.05).

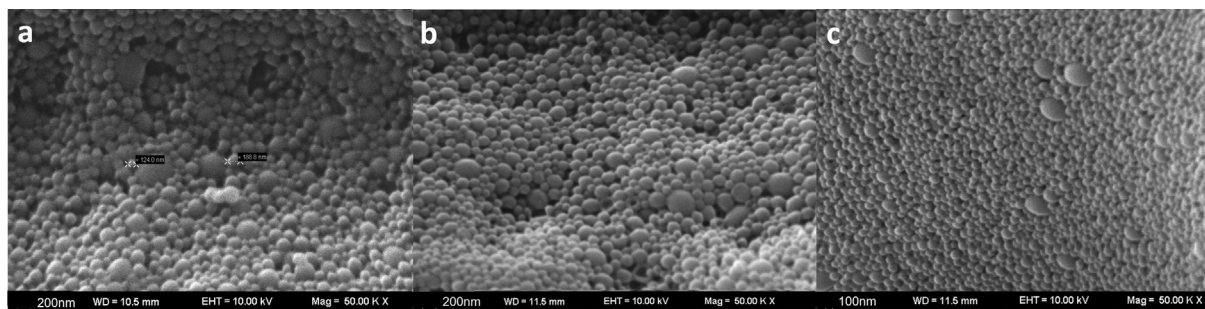


Fig. 1. SEM images of (a) Dox_{NP}, (b) Ver_{NP} and (c) Dox-Ver_{NP}.

over many studies have shown that the smaller particle size has large surface area which, tends to enhance the drug release rate (Alkhaitb and Al-Saedi, 2017).

As shown in Fig. 2, the release rate of the Ver from the Dox-Ver_{NP} were higher than Dox. The drug release from nanoparticles are affected by the structure of the matrix and the solubility of the drug (Qin et al., 2014). The release of Dox from PLGA nanoparticles is a diffusion-dominated process. The interaction of Dox with the nanoparticle matrix causing slower release of Dox from nanoparticles. Moreover, the higher release of Ver from PLGA nanoparticles may be attributed to the higher hydrophilicity of Ver (Alkhaitb and Al-Saedi, 2017).

3.2. Cytotoxicity of formulations

The cytotoxicity of formulations were measured by a real time cell impedance system (xCELLigence, ACEA). The real time cell viability profiles showed that Dox is acting as a DNA-damaging agent (Fig. 3a). The cytotoxic effect of Dox is started 12 h after addition of drug in MCF 7 seeded wells and maximum effect was observed after 24 h. Moreover, concentration dependent effect was observed

as higher concentrations of drug showed higher cytotoxicity. Similar cytotoxicity profiles was observed with previous Dox studies and long periods for observation of cytotoxic effect was explained as DNA-damaging effect of Dox (Moraes et al., 2012).

In vitro cytotoxicity profiles demonstrated that Dox_{NP} which contains the same Dox concentration exhibited lower cytotoxicity than Dox_S (Fig. 3b). As Dox is sequestered inside the nanoparticles, the release of Dox from nanoparticles takes a while and low drug concentrations in wells show less cytotoxic effect. However, it is shown in preclinical studies that particulate Dox systems has higher anticancer activity than Dox solutions. The clearance of Dox nanoparticles is mediated by reticuloendothelial system (RES) which changes the systemic circulation half-life and pharmacokinetics of drug. The application of the same concentration of Dox_{NP} and Dox_S in wells creates an artificial cytotoxicity results strongly favoring Dox_S (Wu et al., 2007).

Fig. 3c shows the dose response profile of MCF 7 to Ver (5 μM to 20 μM) and Dox_S. The Normalised Cell Index after Ver addition reveals that the response of MCF 7 cells to Ver was not concentration dependent at given doses (p > 0.05). The kinetic profiles obtained by the real time cell impedance system showed that the

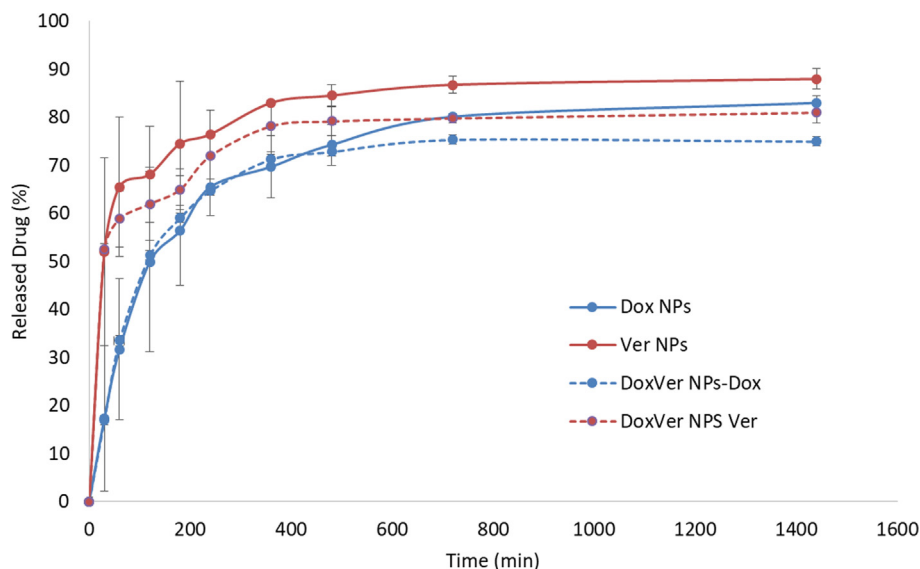


Fig. 2. Drug release from Dox_{NP}, Ver_{NP} and Dox-Ver_{NP}.

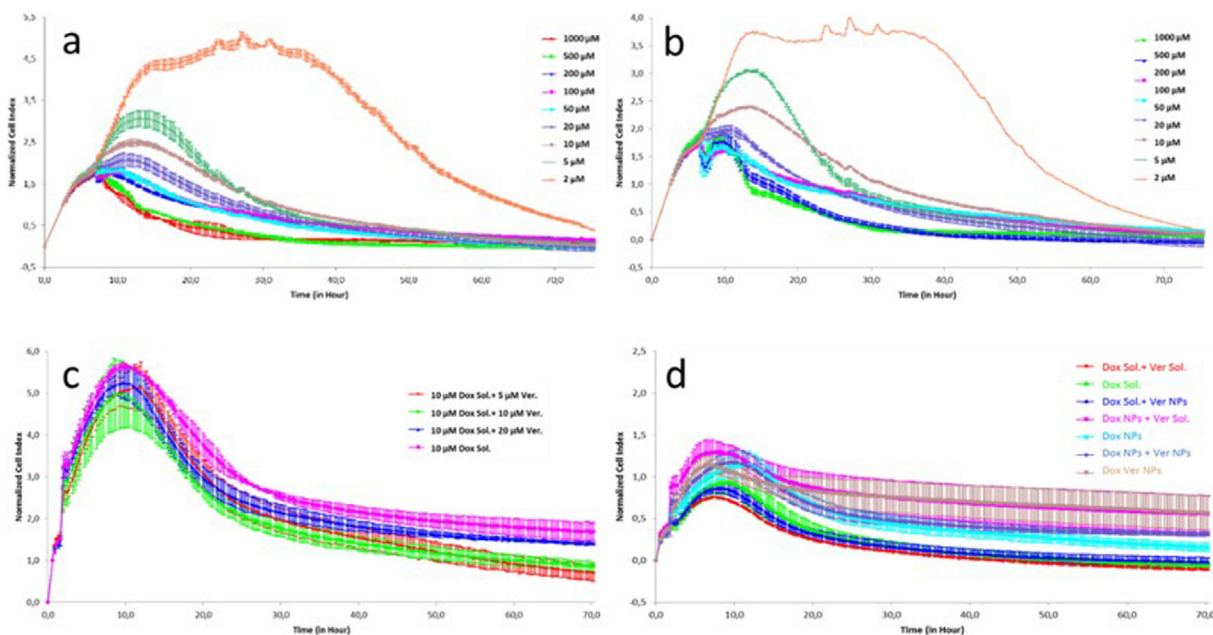


Fig. 3. Dose dependent cytotoxicity of (a) Dox_S and (b) Dox_{NP}. (c) Effect of Ver concentration on Dox cytotoxicity and (d) time dependent cytotoxicity profiles of Dox_S, Dox_{NP}, Dox_S + Ver_S, Dox_S + Ver_{NP}, Dox_{NP} + Ver_{NP} and Dox-Ver_{NP}.

rate and dynamics of cytotoxicity do not vary between the doses ($p > 0.05$). Lai et al. studied different doses of verapamil on doxorubicin and it is explained that the enhanced P-gp inhibition was shown at high concentrations of verapamil (10–80 μmol/L) which is also used in our study (Lai et al., 1993).

The cytotoxicity of several formulations of Dox and Ver on MCF 7 cells were studied. The concentration of Dox (10 μM) was chosen according to previous literature (Wu et al., 2007). As shown in Fig. 3c, the cytotoxic effects of Ver in co-administration with Dox on MCF 7 cells was found concentration dependent between 5 and 20 μM doses. So 10.5 μM concentration of verapamil was chosen for cytotoxicity tests as 10 μM doxorubicin containing Dox-Ver_{NP} also contains 10.5 μM verapamil.

Our results show that cytotoxicity of Dox on MCF 7 cells was higher in solution form than Dox_{NP}. Co-administration of Dox with Ver also did not change this result. The reason of the lower cytotoxicity of Dox_{NP} is encapsulation of drug. Moreover in several studies, it is shown that the IC₅₀ values of particulate Dox was found higher than Dox_S. Yet in the same studies, it is shown that in preclinical studies, Dox particles had higher antitumor activity than Dox solution which is explained as the nanoparticles has longer systemic circulation half-life and particles exhibits fundamentally different pharmacokinetics (Wu et al., 2007).

When the cytotoxicity of Dox_S, Dox_{NP}, Dox_S + Ver_S, Dox_S + Ver_{NP}, Dox_{NP} + Ver_{NP} and Dox-Ver_{NP} were calculated on the same cell line. It was shown that (Fig. 3d) the cytotoxicity of Dox_S + Ver_S was the highest among all formulations. The higher cytotoxicity of Dox_S + Ver_S can be attributed to the combination of the chemosensitizer (Ver) (Qin et al., 2014). It was also shown that nanoparticle administration extended the drug release profile as well as drug release.

3.3. Cellular uptake

It is essential to note that Dox_{NP} and Dox_S have different release properties, which is thought to effect the in vitro cellular uptake. As shown in various articles, the in vivo plasma residence time Dox nanoparticles and Dox solution is different and depending on the surface composition, nanoparticles has a circulation half-life of hours to days, compared to a half-life of minutes for Dox

solution. Hence the given cytotoxicity results cannot be used to compare the effect of solution and nanoparticle formulations of Dox and Ver alone (Wu et al., 2007). However, it is possible to calculate the cellular uptake of drugs in vitro which also can be used to compare the effect of drugs. In this study only cellular uptake of Dox was identified due to cytotoxic effect was dependent to Dox (Wang et al., 2005).

The cell uptake studies showed that both encapsulation in nanoparticles and co administration with Ver changed the Dox uptake by MCF-7 cells ($p < 0.05$) (Fig. 4a,b). Moreover the Dox uptake by MCF 7 cells were increased with longer incubation times and highest drug levels were observed at 4 h incubation ($p < 0.05$). The drug levels in Dox_S, Dox_{NP}, Dox_S + Ver_S, Dox_{NP} + Ver_S, Dox_{NP} + Ver_{NP} and Dox-Ver_{NP} treated cells after 1 h were 31.20%, 11.46%, 19.86%, 5.43%, 7.60% and 3.41% per 10⁵ cells, respectively. After 4 h treatment, the drug levels increased to 64.98%, 35.42%, 70.62%, 50.40%, 70.76% and 36.96% per 10⁵ cells in Dox_S, Dox_{NP}, Dox_S + Ver_S, Dox_{NP} + Ver_S, Dox_{NP} + Ver_{NP} and Dox-Ver_{NP} respectively. At the end of the experiment (4 h), the drug levels of Dox_{NP} + Ver_{NP} was significantly higher compared to Dox_{NP}, Dox_{NP} + Ver_S and Dox-Ver_{NP} treated cells ($p < 0.05$).

The cellular uptake of Dox from Dox_S, Dox_{NP}, Dox_S + Ver_S, Dox_{NP} + Ver_S, Dox_{NP} + Ver_{NP} and Dox-Ver_{NP} formulations were also visualized by Fluorescence microscope (Fig. 5). It was observed that the Dox uptake of nanoparticles was less than drug solution. In case of Dox_{NP} treated cells, the fluorescence intensity changed with the change of Ver administration (Mulik et al., 2010).

3.4. Cell death analysis

The optimal time point to conduct apoptosis assay was estimated using cytotoxicity results obtained by real time cell impedance system. It is explained that the apoptosis tests must be done once the cell index profile reaches its lowest value. Hence 24 h apoptosis analysis were done indicating the lowest level of cell viability.

During the early apoptosis stage, phosphatidylserine is released and Annexin V-FITC can bind to phosphatidylserine with high

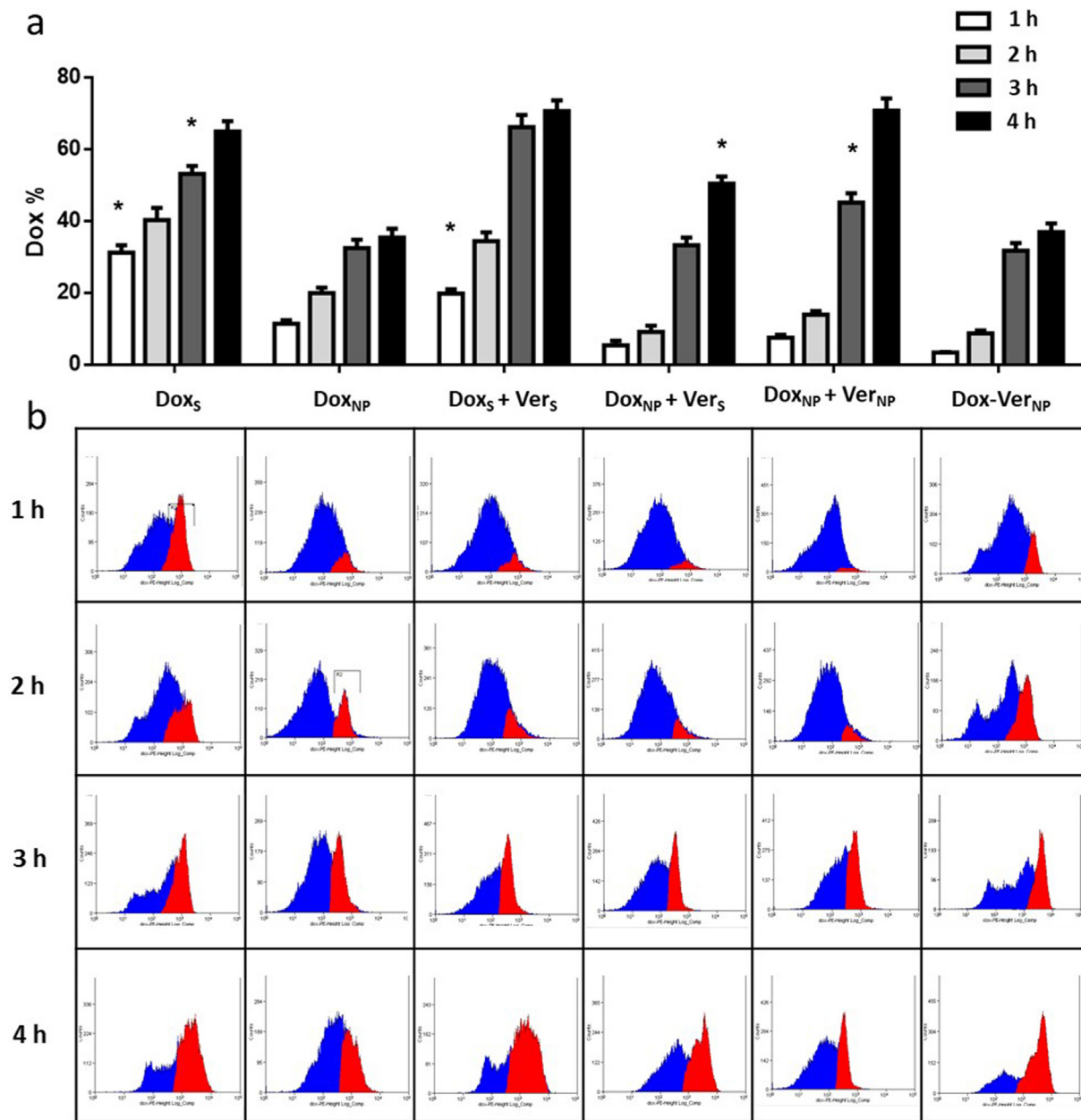


Fig. 4. Bar (a) and flow cytometer (b) results of cell uptake. * shows significant differences ($p < 0.05$).

affinity. Likewise, propidium iodide (PI) can bind to necrotic cells (Mulik et al., 2010).

The induction of apoptosis by Dox and Ver after the treatment with drug solution and nanoparticle was detected and quantified by flow cytometry (Fig. 6). First, the autofluorescence of doxorubicin was checked using treated unstained cells. The apoptotic cells were calculated in cells treated with all formulations but the percentage of apoptotic cells varied with each formulation. Dox_S treated cells showed 1.78% and 12.76% of early apoptotic (AnnexinV-FITC (+) PI (-)) and late apoptotic/early necrotic (AnnexinV-FITC (+) PI (+)) populations, respectively, compared to Dox_S + Ver_S (2.12% and 12.72%), Dox_S + Ver_S (8.66% and 0.32%), DOX_{NP} + Ver_{NP} (13.52% and 52.94%) and Dox-Ver_{NP} (6.25% and 4.23%) treated cells for 24 h. Dox is known to induce apoptosis (Kalyanaraman et al., 2002). It was observed that in all formulations, Dox showed increase in apoptosis correlated with the previous observations obtained with antiproliferative activity and cell uptake study.

Apoptosis study also showed the higher therapeutic potential of DOX_{NP} + Ver_{NP} than Dox_S + Ver_S, Dox_S + Ver_S, and Dox-Ver_{NP} as more apoptosis was detected in DOX_{NP} + Ver_{NP} treated cells compared to all other formulation treated cells. The increase in apoptotic cell death with DOX_{NP} + Ver_{NP} was significantly higher than all formulations ($p < 0.05$). Moreover it is observed that while Dox_S induce necrosis, Dox_{NP} induce apoptosis. This result can be attributed to induction of apoptosis by the PLGA nanoparticles (Kanwar et al., 2012).

4. Conclusion

Our data suggest that the co administration of Dox and Ver enhanced the anticancer activity probably due to high reversal efficacy. Moreover, DOX_{NP} showed that PLGA nanoparticles had a MDR reversal activity on MCF 7 cells. Using PLGA nanoparticles and co-administration of Dox with Ver, numerous strategies for adminis-

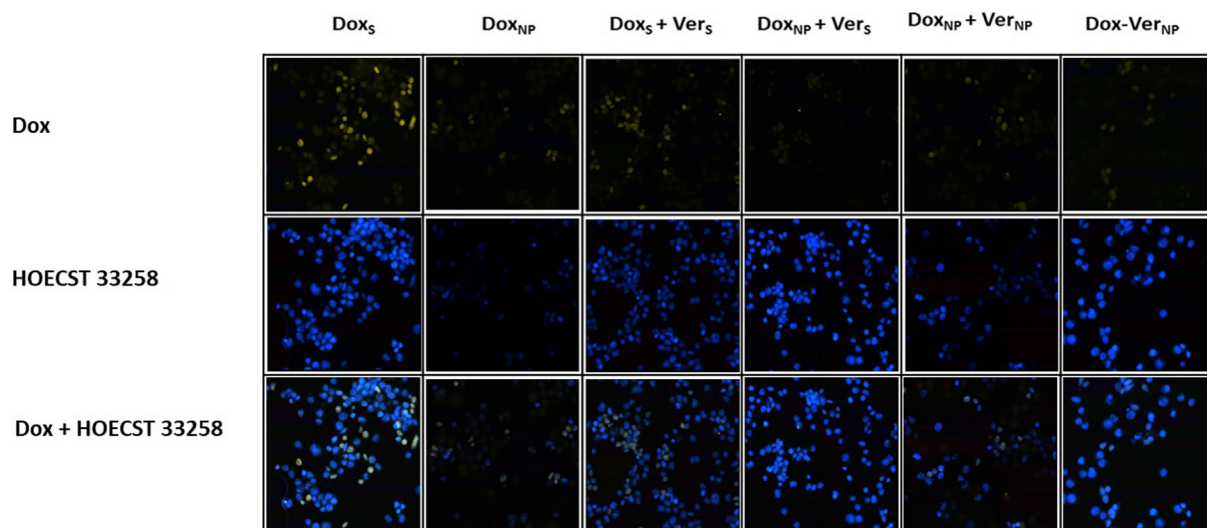


Fig. 5. Fluorescence images of cell uptake study.

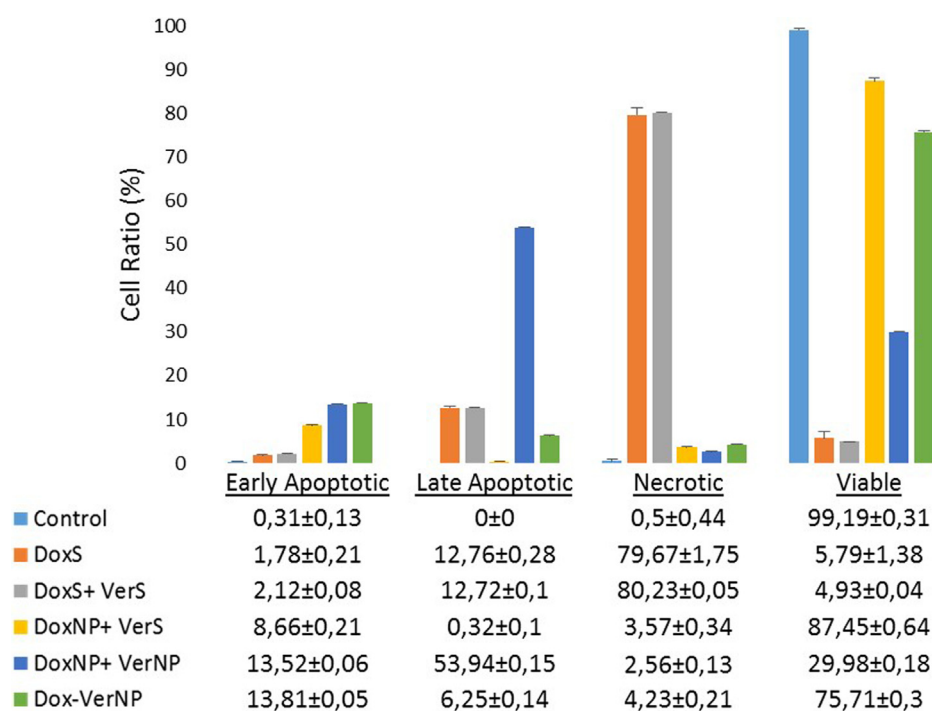


Fig. 6. Cell Death Analysis of Formulations.

tering Dox/Ver combinations were compared. It was found that co administration of Dox_{NP} with Ver_{NP} showed similar cellular uptake of Dox to Dox/Ver combination solution. However it is observed that apoptotic activity of Dox_{NP} was higher than Dox_S and Dox_{NP} + Ver_{NP} has the highest apoptosis induction effect on MCF 7 cells. As described previously, Co-encapsulation of anticancer drug and chemosensitizer might cause lower normal tissue drug toxicity and fewer drug–drug interactions. Hence, it is suggested that Dox_{NP} + Ver_{NP} might be more effective than other formulations.

Declaration of Competing Interest

The authors declare that they have no known competing financial interests or personal relationships that could have appeared to influence the work reported in this paper.

References

- Alkhaitb, M.H., Al-Saedi, D.A., 2017. Cytotoxic effect of the combination of gemcitabine and atorvastatin loaded in nanoparticle on the MCF-7 breast cancer cells and hfs human foreskin cells. *Curr. Nanosci.* 13 (6), 625–633.
- Baek, J.-S., Cho, C.W., 2015. Controlled release and reversal of multidrug resistance by co-encapsulation of paclitaxel and verapamil in solid lipid nanoparticles. *Int. J. Pharm.* 478 (2), 617–624.
- Dönmez, Y., Akhmetova, L., İşeri, Ö.D., Kars, M.D., Gündüz, U., 2011. Effect of MDR modulators verapamil and promethazine on gene expression levels of MDR1 and MRP1 in doxorubicin-resistant MCF-7 cells. *Cancer Chemother. Pharmacol.* 67 (4), 823–828.
- Kalyanaraman, B., Joseph, J., Kalivendi, S., Wang, S., Konorev, E., Kotamraju, S.J., 2002. Doxorubicin-induced apoptosis: implications in cardiotoxicity. *Mol. Cell. Biochem.* 234 (1), 119–124.
- Kanwar, J.R., Kanwar, R.K., Mahidhara, G., Cheung, C.H.A., 2012. Cancer targeted nanoparticles specifically induce apoptosis in cancer cells and spare normal cells. *Aust. J. Chem.* 65 (1), 5–14.

- Kauffman, M.K., Kauffman, M.E., Zhu, H., Jia, Z., Li, Y.R., 2016. Fluorescence-based assays for measuring doxorubicin in biological systems. *Reactive Oxygen Species (Apex, NC)* 2 (6), 432.
- Khdair, A., Handa, H., Mao, G., Panyam, J., 2009. Nanoparticle-mediated combination chemotherapy and photodynamic therapy overcomes tumor drug resistance in vitro. *Eur. J. Pharm. Biopharm.* 71 (2), 214–222.
- Lai, T., Collins, C., Hall, P., Morgan, A., Smith, P., Stonebridge, B., Symes, M., 1993. Verapamil enhances doxorubicin activity in cultured human renal carcinoma cells. *Eur. J. Cancer* 29 (3), 378–383.
- Luo, Y., Ling, Y., Guo, W., Pang, J., Liu, W., Fang, Y., Gao, X., 2010. Docetaxel loaded oleic acid-coated hydroxyapatite nanoparticles enhance the docetaxel-induced apoptosis through activation of caspase-2 in androgen independent prostate cancer cells. *J. Control. Release* 147 (2), 278–288.
- Martinez-Serra, J., Gutierrez, A., Muñoz-Capó, S., Navarro-Palou, M., Ros, T., Amat, J. C., 2014. xCELLigence system for real-time label-free monitoring of growth and viability of cell lines from hematological malignancies. *Oncotargets Therapy* 7, 985.
- Mobarak, D.H., Salah, S., Elkheshen, S.A., 2014. Formulation of ciprofloxacin hydrochloride loaded biodegradable nanoparticles: optimization of technique and process variables. *Pharm. Dev. Technol.* 19 (7), 891–900.
- Moraes, M.C.S., de Andrade, A.Q., Carvalho, H., Guecheva, T., Agnoletto, M.H., Henriques, J.A., Sarasin, A., Stary, A., Saffi, J., Menck, C.F., 2012. Both XPA and DNA polymerase eta are necessary for the repair of doxorubicin-induced DNA lesions. *Cancer Lett.* 314 (1), 108–118.
- Muckova, L., Pejchal, J., Jost, P., Vanova, N., Herman, D., Jun, D., 2019. Cytotoxicity of acetylcholinesterase reactivators evaluated in vitro and its relation to their structure. *Drug Chem. Toxicol.* 42 (3), 252–256.
- Mulik, R.S., Mönkkönen, J., Juvonen, R.O., Mahadik, K.R., Paradkar, A.R., 2010. Transferrin mediated solid lipid nanoparticles containing curcumin: enhanced in vitro anticancer activity by induction of apoptosis. *Int. J. Pharm.* 398 (1–2), 190–203.
- Ozdemir, A., Ark, M., 2013. xCELLigence real time cell analysis system: a new method for cell proliferation and cytotoxicity. *Niche* 2 (2).
- Qin, M., Lee, Y.E.K., Ray, A., Kopelman, R., 2014. Overcoming cancer multidrug resistance by codelivery of doxorubicin and verapamil with hydrogel nanoparticles. *Macromol. Biosci.* 14 (8), 1106–1115.
- Shafiei-Irannejad, V., Samadi, N., Yousefi, B., Salehi, R., Velaei, K., Zarghami, N., 2018. Metformin enhances doxorubicin sensitivity via inhibition of doxorubicin efflux in P-gp-overexpressing MCF-7 cells. *Chem. Biol. Drug Des.* 91 (1), 269–276.
- Song, X.R., Cai, Z., Zheng, Y., He, G., Cui, F.Y., Gong, D.Q., Hou, S.X., Xiong, S.J., Lei, X.J., Wei, Y.Q., 2009. Reversion of multidrug resistance by co-encapsulation of vincristine and verapamil in PLGA nanoparticles. *Eur. J. Pharm. Sci.* 37 (3–4), 300–305.
- Song, X.R., Zheng, Y., He, G., Yang, L., Luo, Y.F., He, Z.Y., Li, S.Z., Li, J.M., Yu, S., Luo, X., Hou, S.X., 2010. Development of PLGA nanoparticles simultaneously loaded with vincristine and verapamil for treatment of hepatocellular carcinoma. *J. Pharm. Sci.* 99 (12), 4874–4879.
- Soni, P., Kaur, J., Tikoo, K., 2015. Dual drug-loaded paclitaxel–thymoquinone nanoparticles for effective breast cancer therapy. *J. Nanopart. Res.* 17 (1), 18.
- Wang, H., Zhao, Y., Wu, Y., Hu, Y.L., Nan, K., Nie, G., Chen, H., 2011. Enhanced anti-tumor efficacy by co-delivery of doxorubicin and paclitaxel with amphiphilic methoxy PEG-PLGA copolymer nanoparticles. *Biomaterials* 32 (32), 8281–8290.
- Wang, J., Goh, B., Lu, W., Zhang, Q., Chang, A., Liu, X.Y., Tan, T.M., Lee, H., 2005. In vitro cytotoxicity of Stealth liposomes co-encapsulating doxorubicin and verapamil on doxorubicin-resistant tumor cells. *Biol. Pharm. Bull.* 28 (5), 822–828.
- Wong, H.L., Bendayan, R., Rauth, A.M., Wu, X.Y., 2004. Development of solid lipid nanoparticles containing ionically complexed chemotherapeutic drugs and chemosensitizers. *J. Pharm. Sci.* 93 (8), 1993–2008.
- Wong, H.L., Bendayan, R., Rauth, A.M., Xue, H.Y., Babakhanian, K., Wu, X.Y., 2006. A mechanistic study of enhanced doxorubicin uptake and retention in multidrug resistant breast cancer cells using a polymer-lipid hybrid nanoparticle system. *J. Pharmacol. Exp. Ther.* 317 (3), 1372–1381.
- Wu, J., Lu, Y., Lee, A., Pan, X., Yang, X., Zhao, X., Lee, R.J., 2007. Reversal of multidrug resistance by transferrin-conjugated liposomes co-encapsulating doxorubicin and verapamil. *J. Pharm. Pharm. Sci.* 10 (3), 350–357.